High-throughput Multiplexed Transcriptome and Protein Measurements in Single Cells

by

Shirin Shivaei

B.S., Massachusetts Institute of Technology (2017)

Submitted to the Department of Electrical Engineering and Computer Science
in partial fulfillment of the requirements for the degree of

Master of Engineering in Electrical Engineering and Computer Science

at the

MASSACHUSETTS INSTITUTE OF TECHNOLOGY

June 2018

©Shirin Shivaei, 2018. All rights reserved.

The author hereby grants MIT permission to reproduce and distribute publicly paper and electronic copies of this thesis document in whole and in part in any medium now known or hereafter created.

Author . . . .
Department of Electrical Engineering and Computer Science
May 30, 2018

Certified by . . . .
Fei Chen
Fellow, Broad Institute of MIT and Harvard
Thesis Supervisor

Accepted by . . . .
Katrina LaCurts
Chair, Master of Engineering Thesis Committee

High-throughput Multiplexed Transcriptome and Protein Measurements in Single Cells

by

Shirin Shivaei

Submitted to the Department of Electrical Engineering and Computer Science
on May 30, 2018, in partial fulfillment of the
requirements for the degree of
Master of Engineering in Electrical Engineering and Computer Science

Abstract

We present cell gels, a platform for high-throughput multiplexed measurements of transcriptome and proteome in single cells. This method takes advantage of droplet barcoding and hydrogel chemistry to capture mRNAs and proteins in thousands of cells. We report the challenges of acquiring sequencing data from cell gels due to complex mechanisms underlying bead based library prep in polyacrylamide gels. We show the applications of this method in detecting intracellular proteins, sorting based on intracellular markers after cell lysis, and expanding thousands of cells in single droplets.

Thesis Supervisor: Fei Chen
Title: Fellow, Broad Institute of MIT and Harvard

Acknowledgments

I would like to first thank my advisor, Fei Chen, for trusting me to independently lead a project in a field I was relatively new to. My experience in the past year made me unbelievably more confident in doing researching, and I owe much of that to Fei. The fast-paced and yet down-to-earth environment that Fei created in our lab enabled me to push my limits much further than I had imagined.

I am very thankful for the mentorship and advice I have received from Evan Macosko. The opportunity to closely interact with him has taught how to do scientific research and pushed me to confidently pursue my goals.

This past year would not have been as nearly enjoyable without the friends I made in the Chen lab. I would like to especially thank Andrew Payne for mentoring me in my early days in the lab, Sam Rodriguez for his helpful advice in navigating research and graduate school applications, Evan Murray for being my consistent climbing buddy, and Linlin Chen for our spontaneous coffee breaks. I will truly miss working and having fun with you all.

I am very grateful to Bob Stickels and Carly Martin for their continuous support and friendship through the ups and downs of my MEng year.

To my MEng Hommies, Deepti, Erin, and Suma, it is perhaps impossible to top the experience of living with you. Thank you for making me laugh even in the worst situations. Let's bring our spirit to the other coast.

To Tiffany, what started as being roommates in our freshman year turned into a lifelong friendship. I am incredibly thankful for your unconditional support, believing in me, and pushing me to dream bigger.

To my uncle's family, thank you for making me part of your family. Because of you, being far away from my home in Tehran was much easier than it could have been.

Finally, I am deeply grateful to my parents for their priceless love and support. No matter how far away we live, you always empower me when I feel down and continue to provide me with the best life advice. And to my sister, Irene, I simply cannot

imagine the past 5 years without you.

I could not have asked for a better MEng experience, and that I owe to the people who made it this amazing. Looking up and forward to the years to come!

Contents

1 Introduction 15

2 Cell Gels Overview 17

3 Microfluidic Device Design, Fabrication, and Operation 21

3.1 Design 21

3.2 Fabrication 22

3.3 Operation 23

3.4 Encapsulation efficiency 24

4 Transcriptome Profiling in Cell Gels 27

4.1 DTT inhibits gelation 27

4.2 DTT alternative: HEPES 28

4.3 DTT alternative: GuHCl 28

4.4 Dissolving gels before amplification 29

4.5 Bead variability 30

4.6 Effect of acrylamide and APS on RNA degradation and reverse transcription 31

5 Protein measurements in cell gels 35

5.1 Antibody staining procedure 35

5.2 FACS sorting 36

5.3 Expanded cell gels 36

6 Discussion **41**

List of Figures

2-1 General workflow of cell gels. Cells are encapsulated with DNA barcoded beads, monomer, and crosslinker, and lysed in aqueous droplets. After droplet collection, TEMED is added to the suspension to begin polymerization, where proteins are also crosslinked to the hyrdrogel matrix. Emulsions are then broken and mRNAs are reverse transcribed. Cell gels can be stained with antibodies, sorted based on intracellular markers, and further processed to create STAMPs for transcriptomic analysis. 18

3-1 Cell gels microfluidic devices designed in AutoCAD a) The initial device adapted from Dropbase (OpenWetWare) has a 50 μm junction, which makes monodisperse cell gels in the range 50-70 μm diameter. b) The final version generates smaller monodisperse cell gels, 35-45 μm in diameter. Addition of passive filters and fluid resistors improves robustness. 22

4-1 Post-RT PCR bioAnalyzer analysis of cell gels made without DTT. (a) 13 cycle PCR, average size 1,811 bps. (b) 16 cycle PCR, average size 1,613 bps. 28

4-2 Comparison of a Drop-seq experiment with AM Biotechnologies (AMBiotech) beads vs. replacing DTT with HEPES (a) Regular Drop-seq, 3000 AMBiotech beads, 16 cycle PCR (b) same experiment with HEPES. 29

4-3 Comparison of a regular Drop-seq experiment and lysis buffer replaced with GuHCl and SSC (a) Regular Drop-seq, 2000 beads, 13 cycle PCR (b) 1.84 M GuHCl, 2x SSC, 3000 Drop-seq beads, 16 cycle PCR. . . . 29

4-4 Effect of dissolving cell gels before amplification on PCR yield: (a) 2.64M GuHCl, 8000 MyOne beads, not dissolved (b) 2.64M GuHCl, 8000 MyOne beads, cell gels dissolved in Exo I buffer before PCR. . . 30

4-5 Comparison of 15 μm AMBiotech beads to regular Drop-seq beads (a) Regular Drop-seq experiment, 2000 Drop-seq beads, 13 cycle PCR. (b) Regular Drop-seq experiment, 3000 AMBiotech beads, 16 cycle PCR. 31

4-6 Analysis of qPCR experiments performed to understand the effect of acrylamide and APS on RNA degradation and RT. Acrylamide and RT did not affect qPCR yields when they were incubated with RNA. Acrylamide also did not affect the yield when it was added to the RT mix. However, RT performed with 0.3% APS and 0.6% APS reduced yields about 10^3 and 10^6 folds respectively. 32

5-1 Staining cell gels with antibodies. Images taken on an epi-fluorescence microscope with 10x magnification, showing the same region of interest in three different wavelengths. Cells gels were stained with DAPI, monoclonal anti-α-Tubulin-Cy3, and monoclonal anti-Tom20-Cy5 conjugated antibodies. (Top) Image taken in 405 nm to detect cell nuclei based on DAPI. (Center) Image taken in 561 nm to detect α-Tubulin. (Bottom) Image taken in 640 nm to detect Tom20. 37

5-2 Cell gels stained with DAPI and sorted on FACS. The green area consists of cell gels that encapsulated a cell, showing a population enrichment of 4.59%. 38

5-3 Image of a cell gel encapsulating a cell in 405 nm. Cell gels were collected after sorting on FACS. The population was successfully sorted to cell gels containing cells and empty cell gels. 38

5-4 Cell gels expanded 4x and stained with intracellular markers. (Top) DAPI in blue and Histone H3 in magenta (Bottom) DAPI in blue and Histone H4 in red. 39

List of Tables

3.1 Spin coat settings to make 30 μm deep microfluidic channels with SU-8 2025 photoresist. 22

4.1 Summary of experiments to improve transcriptome library prep in cell gels. 32

4.2 List of beads and their oligo sequences. 33

Chapter 1

Introduction

The unbiased and high-throughput nature of modern single-cell RNA-seq (scRNA-seq) methods [8, 11, 21] have revolutionized our definition of heterogeneity in diverse cell populations. Prior to the evolution of these methods, probing cellular heterogeneity mainly relied on staining for specific known proteins via multi-colour flow cytometry and fluorescent conjugated monoclonal antibodies. scRNA-seq methods enabled us to use genetic information to cluster thousands of cells based on their genetic expression patterns without a priori knowledge about expression levels. These methods have resulted in the discovery of new or rare cell types [19], enabled a deeper understanding of mechanisms underlying cell proliferation and development [14], and enhanced our ability to probe the cellular ecosystem of diseases [18].

However, scRNA-seq methods produce one-dimensional genetic information on cellular diversity: the ability to capture the transcriptome of thousands of cells is only the first step towards a comprehensive understanding of cellular heterogeneity and phenotypic variations. mRNA expression levels are not sufficient to predict protein abundance due to temporal and spatial variations of mRNA transcription, local availability of resources for protein translation [10], and post-transnational protein modifications [3]. Additionally, proteins are the ultimate target of therapeutics and can more accurately predict response to treatments [6]. Thus, genetic information alone is not enough to completely understand and predict biological processes.

Recent methods have attempted to leverage high-throughput single cell technologies to capture proteins in addition to the transcriptome [16, 13, 7][4, 5, 6]. These methods are able to target cell surface markers but they lack accessibility to intracellular proteins. Here, we present a droplet-based method that enables high-throughput multiplexed mRNA and protein measurements in single cells. Our approach, which we call “cell gels”, takes advantage of hydrogel chemistry to capture proteins in droplets and DNA barcoded beads to capture the transcriptome of single cells with unique barcodes that can be mapped back to the cell of origin.

Chapter 2

Cell Gels Overview

The novelty of cell gels is in combining hydrogel chemistry with droplet-based single cell methods to capture multiplexed molecular information. In cell gels, we encapsulate live cells with lysis buffer, monomer, crosslinker, polymerization initiator, and DNA barcoded beads in droplets, picoliter aqueous compartments suspended in oil (see Figure 2-1). Cells are lysed seconds after droplet formation with their mRNA hybridized to the bead in each droplet. After all droplets are collected, a catalyst (TEMED) is added to the suspension to initiate polymerization. Within minutes, aqueous droplets turn into hydrogels that contain mRNAs hybridized to the beads and proteins crosslinked to the hydrogel matrix.

The transcriptome is captured via DNA barcoded beads, consisting of thousands of oligonucleotides attached to polystyrene based microparticles, synthesized via split-and-pool to create millions of distinct cell barcodes. The oligonucleotides include 1) a PCR handle constant on all beads 2) a cell barcode unique to each bead 3) a Unique Molecular Identifier (UMI) different on each oligonucleotide on the bead, used to identify PCR duplicates and 4) oligo-dT sequence (T30) on the 3'end to capture polyadenylated mRNAs.

Meanwhile, proteins of lysed cells are crosslinked to the matrix of the acrylamide hydrogel using acryloyl-X (AcX). The succinimidyl ester of acryloyl-X, SE (6-((acryloyl)amino) hexanoic acid) reacts with amines of proteins to yield acrylamides that can be copolymerized into the polyacrylamide matrix of an acrylamide

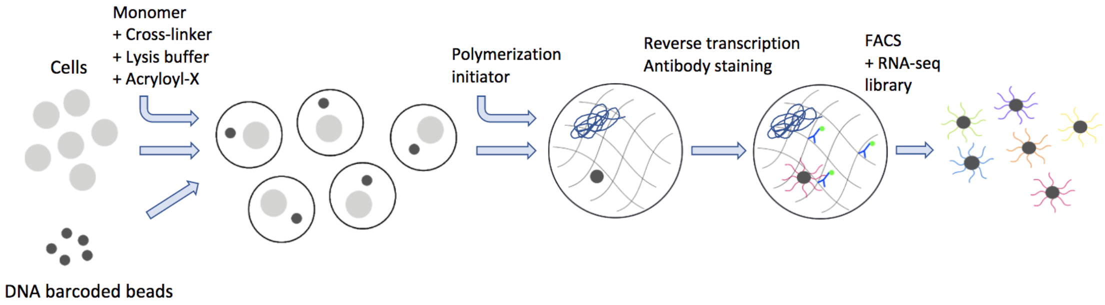

Figure 2-1: General workflow of cell gels. Cells are encapsulated with DNA barcoded beads, monomer, and crosslinker, and lysed in aqueous droplets. After droplet collection, TEMED is added to the suspension to begin polymerization, where proteins are also crosslinked to the hyrdrogel matrix. Emulsions are then broken and mRNAs are reverse transcribed. Cell gels can be stained with antibodies, sorted based on intracellular markers, and further processed to create STAMPs for transcriptomic analysis.

gel. Therefore, AcX functions as a crosslinker between the polyacrylamide matrix and amines of proteins. We assume that by saturating with AcX, we are able to capture the proteome, including intracellular proteins and cell surface markers, in cell gels.

In our experiments, live cells were washed once in 1x PBS and resuspended to 6-8 million cells per mL in a total volume of 500 μL 1X PBS and 4% ficoll. Cells were then encapsulated with lysis buffer, 10% acrylamide monomer and crosslinker, 0.6% ammonium persulfate (APS), 0.2 mg/mL Acrylol-X (AcX) and beads in aqueous droplets in oil (QX200 droplet generation oil for EvaGreen, BioRad Inc.). Immediately after droplet formation, mRNAs are hybridized to the beads. Droplets were collected for about 30 min and incubated with 1% TEMED in vacuum for 15 min for polymerization to terminate. Emulsions were broken in 300 uL of perfluorooctanol in a 15 mL tube filled with 3x SSC, 0.1 mM EDTA, 0.01% Triton X-100, and washed once with the same buffer.

Immediately after droplet breakage, the mRNAs were reverse transcribed in bulk, forming STAMPs (single-cell transcriptomes attached to microparticles. Template switching was used to introduce a PCR handle downstream of the the synthesized cDNA [22] which is amplified with SMART PCR primers. As described in Chapter

4, we conducted different experiments to compare PCR amplification done in cell gels versus dissolving gels first before amplifying. The amplified DNA was purified and pooled with AMPure XP beads. The amplified product was quantified on a high-sensitivity DNA chip on Agilent 2100 bioAnalyzer. The amplified cDNA was fragmented and amplified for sequencing on an Illumina platform with the Nextera XT DNA sample prep kit (Illumina) and indexed primers. The sequencing results were analyzed on the Zamboni platform.

Chapter 3

Microfluidic Device Design, Fabrication, and Operation

3.1 Design

The design of the microfluidic device used to generate cell gels is indicated in Figure 3-1. The device contains three inlets for i) cell suspension ii) barcoded beads, lysis buffer, monomer, crosslinker, and initiator iii) carrier oil, and one outlet for droplet collection. To reduce flow fluctuations due to the mechanics of the syringe pumps, the device has fluid resistors with a serpentine shape. The cell suspension inlet and the oil inlet contain passive filters that prevent PDMS collapse [9] and also prevent channels from clogging. The device consists of two junctions, one for bringing the two aqueous inputs together, and one where aqueous and oil phases meet and form water-in-oil (w/o) emulsions. The aqueous-aqueous junction is in shape of a Y-junction that allows aqueous inputs to form two laminar flows in one channel. Due to a difference in fluid viscosity, the aqueous streams do not combine until they form w/o emulsions. The aqueous-oil junction consists of a 26 μm flow focusing channel than opens into a 35 μm channel. The flow-focusing geometry enables making monodisperse droplets whose size is determined by the diameter of the focused stream and are typically much smaller than the orifice [2]. We successfully made monodisperse cell gels as small as 35 μm after 1.4x expansion post gelation.

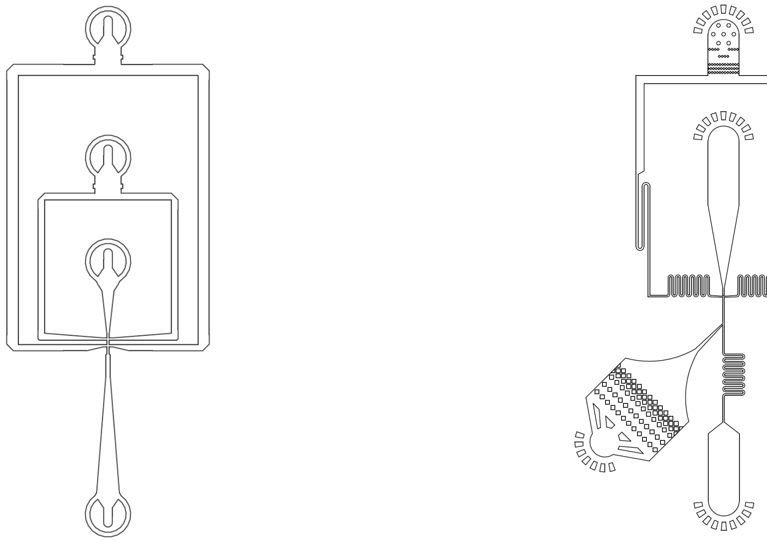

(a) Initial design (b) Final design

Figure 3-1: Cell gels microfluidic devices designed in AutoCAD a) The initial device adapted from Dropbase (OpenWetWare) has a 50 μm junction, which makes monodisperse cell gels in the range 50-70 μm diameter. b) The final version generates smaller monodisperse cell gels, 35-45 μm in diameter. Addition of passive filters and fluid resistors improves robustness.

3.2 Fabrication

Microfluidic devices were designed in AutoCAD 2015 and printed on high precision photomasks (CAD/Art Services, Inc.). The device in Figure 3-1b with rectangular channels 30 μm deep was manufactured based on protocols reported previously [12, 1]. Briefly, a 3-inch silicon wafer was spin coated with SU-8 2025 photoresist (MicroChem, MA) with settings indicated in Table 3.1. RPM2 can be decreased for a shallower channel depth and increased for more depth.

RPM1	Time1 [sec]	Accel1	RPM2	Time2 [sec]	Accel2
500	20	1000	1250	60	3000

Table 3.1: Spin coat settings to make 30 μm deep microfluidic channels with SU-8 2025 photoresist.

A spin coated silicon wafer was baked at 65 C for 1 min, 95 C for 4 min, 65 C for 1 min, exposed to UV light for 7 sec and 3 sec consecutively through the mask having a design indicated in Figure 3-1b, and baked at 65 C for 1 min, 95 C for 5 min, and 65 C for 1 min. Silicon wafer was rinsed with SU-8 developer, acetone, and isopropanol and dried on a 150 C for 5 min. The wafer was exposed to a few drops of evaporating silane (TriMethylChloroSilane) for 15 min to make the surface hydrophobic.

Polydimethylsiloxane (PDMS) base and cross-linker were mixed at 10:1 ratio and about 30 mL poured into a Petri dish containing a developed silicon wafer. The PDMS was degassed for at least 30 min, and incubated overnight at 80 C. The PDMS layer was then peeled-off and inlet-outlet ports were punched with a 1 mm biopsy punch (Harris Uni Core). The patterned side of PDMS and a glass slide were treated with oxygen plasma for 50 sec and attached together. The device was baked for 20 min at 80 C to enhance bonding. To render the channels hydrophobic, the device was treated with Aquapel (Pittsburgh Glass Works Inc., Pittsburgh, PA) following a previously developed protocol [11].

3.3 Operation

Cell suspension and bead/lysis/monomer solution were placed in 1 mL glass syringes (BD). Carrier oil (QX200 Droplet Generation Oil for EvaGreen, BioRad) was filtered with a 0.2 μm filter and placed in a 3 mL plastic syringe (BD). Each phase was injected into the microfluidic device via polyethylene tubing (0.015” I.D. x 0.043” O.D.) and needle (a 26G x 1/2). We used 100 μL/hr flow rate for the aqueous inputs and 500 μL/hr for oil to generate 8 pL droplets at a frequency of approximately 5000 droplets per second based on Equation 3.1:

$$f = \frac{Q_d}{V_d} \tag{3.1}$$

Where Q_d is flow rate of the dispersed phase, V_d is droplet volume and f is frequency of droplet generation [4]. Based on our experiments, 100:500 (aqueous:oil) flow rates minimized droplet size while maintaining monodispersity. A higher Q_c/Q_d ratio (where Q_c is flow rate of the carrier oil) resulted in polydisperse droplets. A very large Q_c would result in a jetting stream, while smaller flow rates could be used to generate larger droplets. Overall, droplet size and dispersity depend on flow rates and viscosities of the streams and should be optimized for every experiment.

Droplets were collected in a 1.5 mL tube for about 30 min on ice. After collection, 1% TEMED was added to the suspension, pipetted 10-15 times and incubated in vacuum for 15 min to allow for gelation. Carrier oil (bottom layer) was removed from the tube. Emulsions were then resuspended in 3x SSC, 0.1 mM EDTA, 0.01% Triton X-100 (wash buffer) and moved to a 15 mL tube. The tube was filled with the wash buffer and 300 μL of 1H,1H,2H,2H-Perfluoro-1-octanol (PFO) to break emulsions. The large buffer volume is required to stop hybridization and prevent secondary and tertiary structures from forming on the beads. Suspension was vortexed and centrifuged at 5000 RCF for 2 min. Supernatant (top layer) and PFO (bottom layer) were taken out. 10 mL of the wash buffer was added, vortexed, and centrifuged at 3000 RCF for 5 min. At this point, cell gels are ready for downstream processing of DNA, RNA, and protein.

3.4 Encapsulation efficiency

The number of cells or beads inside each droplet can be estimated with the Poisson distribution [15], in which probability of finding x cells or beads per droplet is given by Equation 3.2:

$$P(X = x) = \frac{\lambda^x e^{-\lambda}}{x!} \tag{3.2}$$

Where λ represents mean number of cells (or beads) in the volume of each droplet. Assuming that encapsulating a cell and a bead are independent events, probability of co-encapsulating x_1 cells and x_2 beads in a single droplet is given by Equation 3.3:

$$P(X_1 = x_1, X_2 = x_2) = \frac{\lambda_1^{x_1} e^{-\lambda_1}}{x_1!} \frac{\lambda_2^{x_2} e^{-\lambda_2}}{x_2!} \tag{3.3}$$

The co-encapsulation efficiency of cells and beads is then,

$$P(X_1 \geq 1, X_2 \geq 1) = (1 - e^{-\lambda_1})(1 - e^{-\lambda_2}). \tag{3.4}$$

With 8 pL droplets and $6x10^6$ cells (or beads) per mL, *lambda* is approximately 0.048. The encapsulation efficiency of a cell (or a bead) per droplet is therefore 4.6% and the co-encapsulation efficiency is 0.22%. Although the efficiency of our experiments was low, we found that increasing the concentration of cells or beads could clog microfluidic channels and result in inconsistency among experiments. The current concentrations are chosen to avoid such errors.

Chapter 4

Transcriptome Profiling in Cell Gels

The general approach to capture and sequence mRNAs in cell gels is described in Chapter 2. Overall, our experiments showed low PCR yields and short sequencing reads, making it challenging to acquire reliable transcriptome information. This chapter describes experiments conducted to understand mechanisms that interfered with library preps and attempts to resolve the problems. Experiments are briefly summarized in Table 4.1.

4.1 DTT inhibits gelation

Initially, the lysis buffer used in making cell gels contained 300 mM NaCl, 20 mM DTT, 2 mM EDTA, and 40 mM Tris-HCl pH 7.5, 2% Sarkosyl, 10% monomer-crosslinker, 1.2% APS. After multiple experiments with and without DTT, we found that the addition of DTT prevents polymerization. DTT is used to reduce RNase activity by preventing formation of disulfide bonds in RNAse [5]. However, it can also reduce the disulfide bridge of a polymer and break apart the matrix of a polyacrylamide gel.

Without replacing DTT, we attempted generating cell gels from a K562 cell line and sequencing them. Although the post-PCR product was promising (Figure 4-1), sequencing reads were too short, suggesting that the sequencing primer fell during ligation. Additionally, repeat experiments to reproduce the same results failed at the cDNA amplification step.

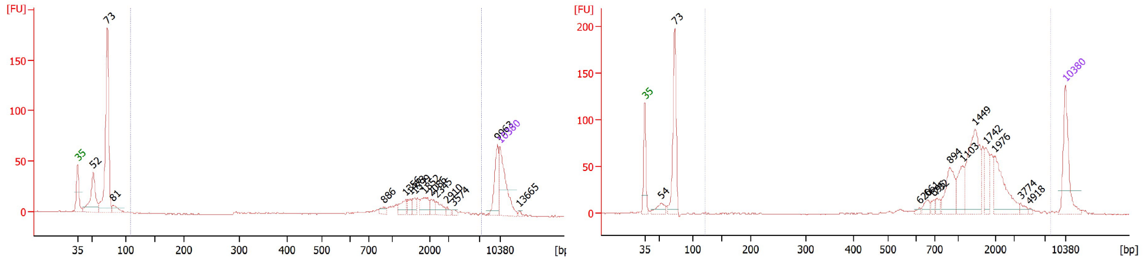

(a) 13 cycle PCR

(b) 16 cycle PCR

Figure 4-1: Post-RT PCR bioAnalyzer analysis of cell gels made without DTT. (a) 13 cycle PCR, average size 1,811 bps. (b) 16 cycle PCR, average size 1,613 bps.

As DTT is essential for inhibiting RNAses, we focused on compensating for its elimination by using HEPES and guanidinium hydrochloride (GuHCl), as described below.

4.2 DTT alternative: HEPES

HEPES is commonly used in the storage buffer of RNAse inhibitors. HEPES also easily forms free radicals and therefore catalyzes the rate of polymerization. Although HEPES improved PCR yield after RT of beads without gelation (see Figure 4-2, we found that replacing DTT by HEPES made the lysis buffer gel before we started the droplet generation process. Therefore, HEPES is not suitable for use in cell gels.

4.3 DTT alternative: GuHCl

We replaced DTT with GuHCl which reduces enzymatic activity of RNAse. To increase molarity of GuHCl, we replaced the regular lysis/hybridization buffer by 20 mM EDTA, 2% Sarkosyl, 2x SSC, 10% acrylamide monomer and crosslinker, 0.6% APS, and 1.84 M GuHCl. Adding GuHCl improved amplification yields, as shown in Figure 4-3.

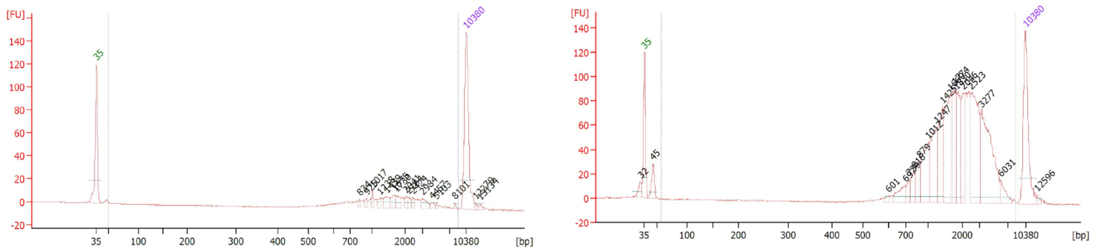

(a) (b)

Figure 4-2: Comparison of a Drop-seq experiment with AM Biotechnologies (AM-Biotech) beads vs. replacing DTT with HEPES (a) Regular Drop-seq, 3000 AM-Biotech beads, 16 cycle PCR (b) same experiment with HEPES.

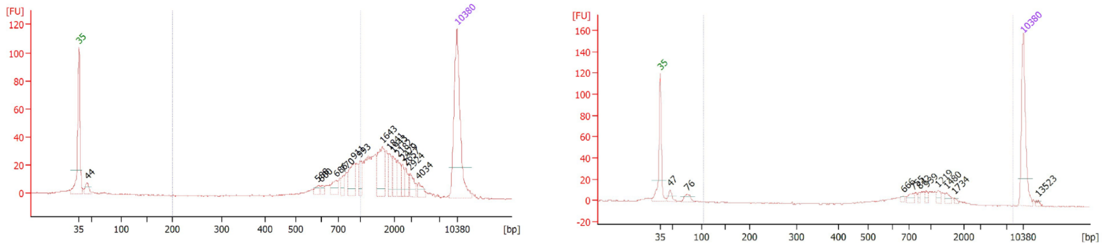

(a) (b)

Figure 4-3: Comparison of a regular Drop-seq experiment and lysis buffer replaced with GuHCl and SSC (a) Regular Drop-seq, 2000 beads, 13 cycle PCR (b) 1.84 M GuHCl, 2x SSC, 3000 Drop-seq beads, 16 cycle PCR.

4.4 Dissolving gels before amplification

Next, we wanted to investigate whether dissolving the polyacrylamide gel before PCR would enhance amplification. For these experiments, we used DHEBA as a crosslinker and found that a 45 min incubation at 42 C in 1x Exo I buffer, 8.3 mM EDTA, and 0.1% Triton X-100 dissolves gels completely. Exo I buffer contains 2-mercaptoeth which is a strong reducing agent that cleaves disulfide bonds and can dissolve polyacrylamide gels. As shown in Figure 4-4, dissolving gels significantly reduces the amount of amplified DNA. Additionally, in the control condition (undissolved gels), the average DNA size is shifted left to 742 bps, while in a high-quality library the average size should be 1,300 - 2,000 bps. These results suggest that we may be non-specifically amplifying DNA trapped in the gel instead of amplifying cDNAs hybridized to the beads. It is worth noting that in these experiments, we increased the molarity of GuHCl to 2.64 M by replacing SSC with GuHCl. These experiments were performed with custom oligo-conjugated MyOne Carboxylic Acid Dynabeads, consisting of a truncated TruSeq Universal Adapter, UMI, and oligo(dT) (see Table 4.2 for the sequence). However, these cell gels were reverse transcribed only with a SMART PCR primer, suggesting that we did not amplify both ends of the cDNAs and mainly captured genomic DNA.

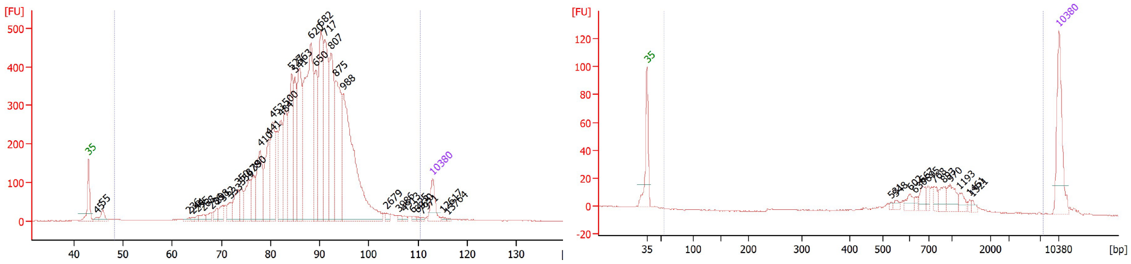

(a)

(b)

Figure 4-4: Effect of dissolving cell gels before amplification on PCR yield: (a) 2.64M GuHCl, 8000 MyOne beads, not dissolved (b) 2.64M GuHCl, 8000 MyOne beads, cell gels dissolved in Exo I buffer before PCR.

4.5 Bead variability

In our experiments, we used the regular Drop-seq beads (ChemGenes, MA), smaller beads with a similar oligo structure (ChemGenes, MA and AM Biotechnologies) as specified in Table 4.2. The original Drop-seq beads were used as control with the Drop-seq device, but they were too large in size to be suitable for our 30 μm device. Instead, we used 15 μm polystyrene beads with the same oligo (AM Biotechnologies). As shown in Figure 4-5, we found that regular Drop-seq beads have better yields than AMBiotech beads.

We also experimented with 10 μm beads from ChemGenes which formed large clumps as they flowed through the microfluidic device and clogged the channels quickly.

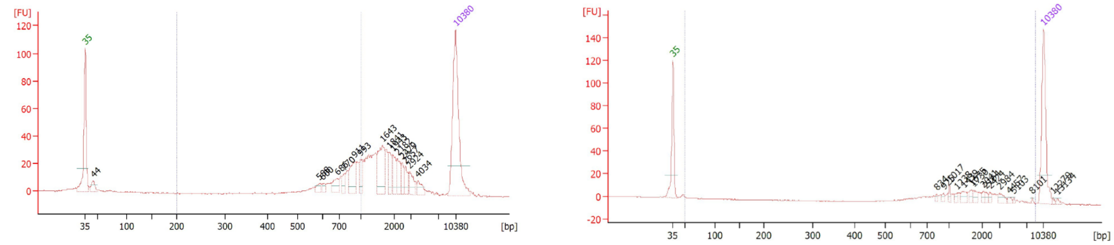

(a) (b)

Figure 4-5: Comparison of 15 μm AMBiotech beads to regular Drop-seq beads (a) Regular Drop-seq experiment, 2000 Drop-seq beads, 13 cycle PCR. (b) Regular Drop-seq experiment, 3000 AMBiotech beads, 16 cycle PCR.

4.6 Effect of acrylamide and APS on RNA degradation and reverse transcription

We performed the following experiments with soluble RNA to understand the effect of acrylamide and APS on RNA degradation and RT. In one set of experiments, we incubated RNA with acrylamide and/or APS for 15 min on ice, conducted RT in bulk, and amplified with qPCR. In a second set of experiments, we combined soluble RNA with acrylamide and/or APS and the RT mix all at once, reverse transcribed, and then amplified with qPCR. The concentrations of reagents other than APS were equal to the final concentrations in cell gels. APS concentration was varied from 0 to 0.6%. As shown in Figure 4-6, acrylamide and APS did not affect RNA degradation. Acrylamide also did not affect RT significantly. However, qPCR yields were correlated negatively with APS concentrations, when APS was added to the RT mix.

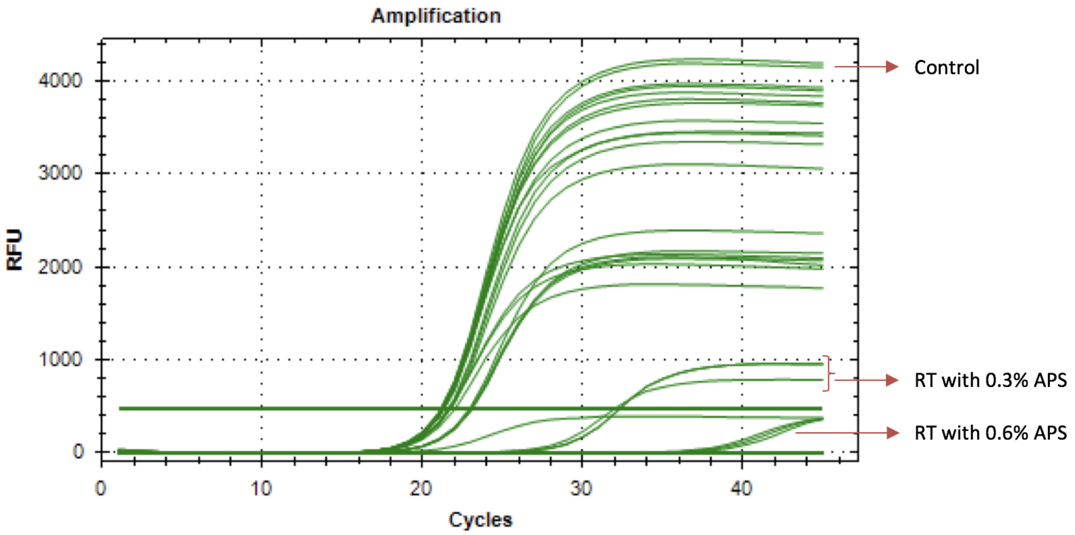

Figure 4-6: Analysis of qPCR experiments performed to understand the effect of acrylamide and APS on RNA degradation and RT. Acrylamide and RT did not affect qPCR yields when they were incubated with RNA. Acrylamide also did not affect the yield when it was added to the RT mix. However, RT performed with 0.3% APS and 0.6% APS reduced yields about 10^3 and 10^6 folds respectively.

Section	**Condition**	**Result**
All	Regular Drop-seq	Control
4.1	20 mM DTT in lysis/hyb/monomer buffer	DTT inhibits gelation.
4.2	Replacing DTT with HEPES	HEPES causes premature gelation.
4.3	Replacing DTT with 1.84 M GuHCl	Improves RNA stability compared to the negative control, but cDNA amplification yield is less than Drop-seq.
4.4	Dissolving gels before cDNA amplification	Significantly reduces PCR yield, suggesting non-specific amplification of genomic DNA.
4.5	Capture efficiency of AMBiotech beads vs. Drop-seq beads	AMBiotech beads have less capture efficiency.
4.5	ChemGene beads vs. Drop-seq beads	ChemGene beads are sticky and clog channels.

Table 4.1: Summary of experiments to improve transcriptome library prep in cell gels.

Bead	**Oligo sequence**
Drop-seq	5’-Bead-linker-TTTTTTTAAGCAGTGGTATCAACGCAGAGTACJJJJJJJJJJJJNNNNNNNNTTTTTTTTTTTTTTTTTTTTTTTTTTTTTT-3’
AM Biotechnologies	5’-Bead-linker-TTTT[dU][dU]AAGCAGTGGTATCAACGCAGAGTACJJJJJJTCTTCAGCGTTCCCGAGJJJJJJNNNNNNNNTTTTTTTTTTTTTTTTTTTTTTT-3’
ChemGenes	5’-Bead-linker-TTTT[dU][dU]AAGCAGTGGTATCAACGCAGAGTACJJJJJJTCTTCAGCGTTCCCGAGJJJJJJNNNNNNNNTTTTTTTTTTTTTTTTTTTTTTT-3’
MyOne Dynabeads	5’-Bead-linker-TTTTTTTCTACACGACGCTCTTCCGATCNNNNNNNNTTTTTTTTTTTTTTTTTTTTTTTTTTTTTTT-3’
Sera-Mag Oligo(dT)-coated magnetic beads	5’-Bead-linker-TTTTTTTTTTTTTT-3’

Table 4.2: List of beads and their oligo sequences.

Chapter 5

Protein measurements in cell gels

Polymerization of droplets allows us to capture both intracellular proteins and cell surface markers by crosslinking them to the polymer matrix of a cell gel via amine-reactive probes, such as acryloyl-X SE. We found that proteins are stably crosslinked, can be detected with antibodies, and used for cell sorting.

5.1 Antibody staining procedure

We incubated cell gels in primary antibodies diluted to 1:100 in 1x PBS and 0.1% Triton X-100 (PBST). Cell gels were washed 3x in PBST and incubated for 1 hr in a secondary fluorophore conjugated antibody diluted 1:100 in PBST. Cell gels were washed 3 times in PBST and imaged with a standard epi-fluorescence microscope or a confocal microscope, depending on the resolution required.

We stained cell gels with Cox IV (mitochondrial transmembrane protein), α-Tubulin (microtubule protein), Histone H3, and Tom20 (mitochondrial outer membrane protein) rabbit antibodies. Cell gels were also incubated in DAPI diluted 1:1000 in PBS for 5 min and washed 3 times in PBST. Figure 5-1 shows images from some of these experiments, a proof of concept that cell gels successfully capture intracellular proteins.

5.2 FACS sorting

On of the benefits of cell gels is that it allows sorting cells based on intracellular markers with a fluorescence activated cell sorter (FACS) even after cell lysis. To show this capability, we sorted cell gels on DAPI. Figure 5-2 shows a 4.59% population enrichment, which is very close to the expected encapsulation efficiency of cell gels (4.6%) based on a Poisson distribution. Additionally, the enriched cell gels, cell gels that encapsulated a cell and were fluorescent in DAPI emission wavelength, were collected after sorting as shown in Figure 5-3.

5.3 Expanded cell gels

Expandable cell gels can enable high resolution imaging and better enzymatic reactions. By using poly-acrylate as the gel matrix, we were able to expand cell gels by 4x in volume.

K562 cells were resuspended in 1X PBS at 4C and fixed with cold 4% PFA for 10 min at room temperature. Cells were then washed with 1X PBS and 100 mM glycine for 5 min to quench fixation and washed twice in 1X PBS, each time for 5 min. Cells were then permeabalized in 1X PBS and 0.1% Triton X-100 at room temperature for 15 min, washed with 1X PBS, and resuspended in 1.06X monomer solution, as reported previously [17]). The lysis/bead solution was replaced with 0.6% APS and 0.2 mg/μL acrylol-X SE, brought up to 500 μL by 1.06X monomer solution. The final monomer solution per droplet was 1.04X.

Droplets were generated, gelled, and broken as describe in Chapter 2. After droplet breakage, cell gels were incubated in water 3 times, each time for 1 hour to allow swelling. Expanded cell gels were then stained with DAPI, Histone H3 and Histone H4 monoclonal antibodies, and Alexa Flour 647 nm conjugated secondary antibody. Stained cell gels were imaged with 10X and 40X magnification as shown in Figure 5-4. Cell gels expanded 4X in volume.

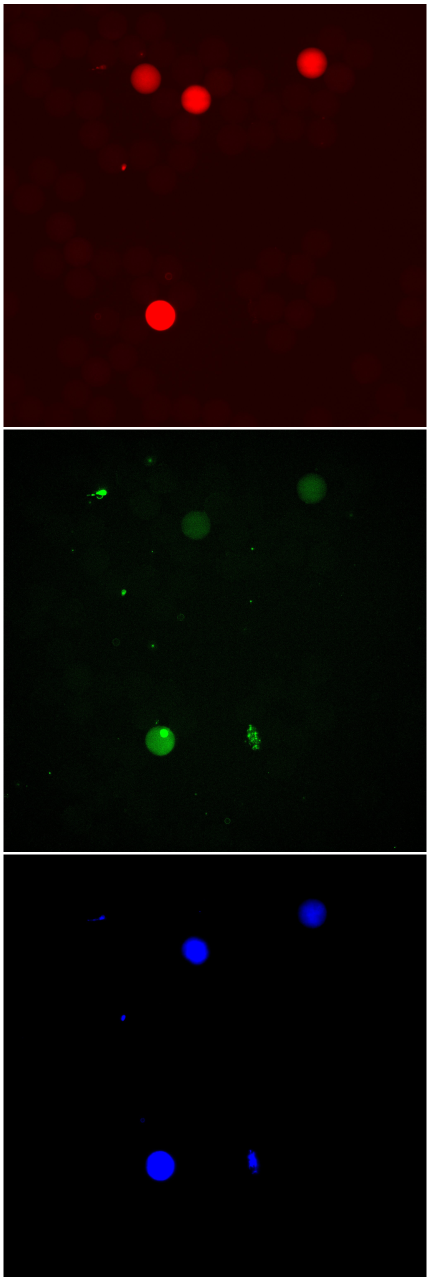

Figure 5-1: Staining cell gels with antibodies. Images taken on an epi-fluorescence microscope with 10x magnification, showing the same region of interest in three different wavelengths. Cells gels were stained with DAPI, monoclonal anti-α-Tubulin-Cy3, and monoclonal anti-Tom20-Cy5 conjugated antibodies. (Top) Image taken in 405 nm to detect cell nuclei based on DAPI. (Center) Image taken in 561 nm to detect α-Tubulin. (Bottom) Image taken in 640 nm to detect Tom20.

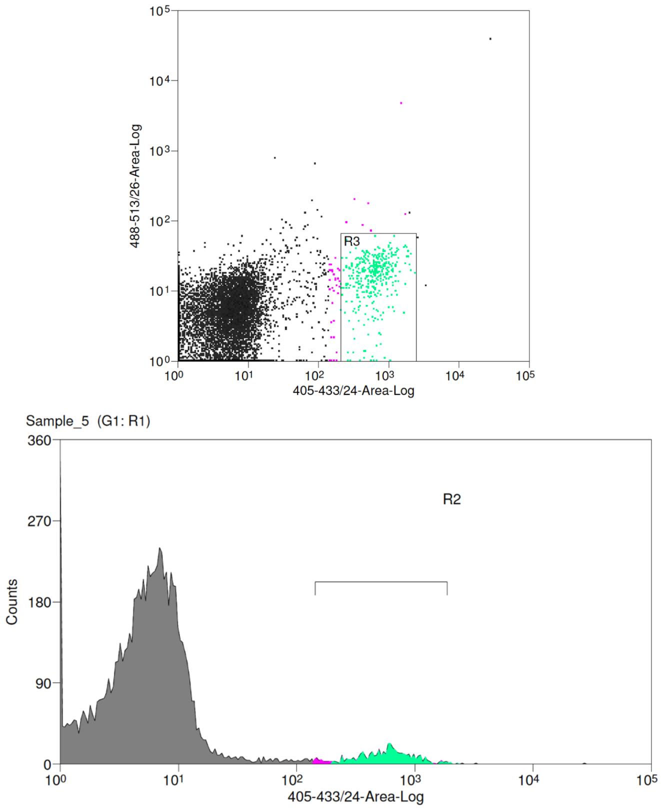

Figure 5-2: Cell gels stained with DAPI and sorted on FACS. The green area consists of cell gels that encapsulated a cell, showing a population enrichment of 4.59%.

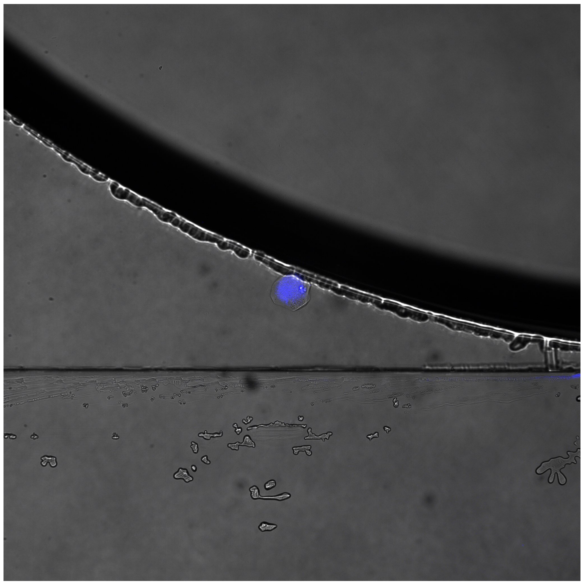

Figure 5-3: Image of a cell gel encapsulating a cell in 405 nm. Cell gels were collected after sorting on FACS. The population was successfully sorted to cell gels containing cells and empty cell gels.

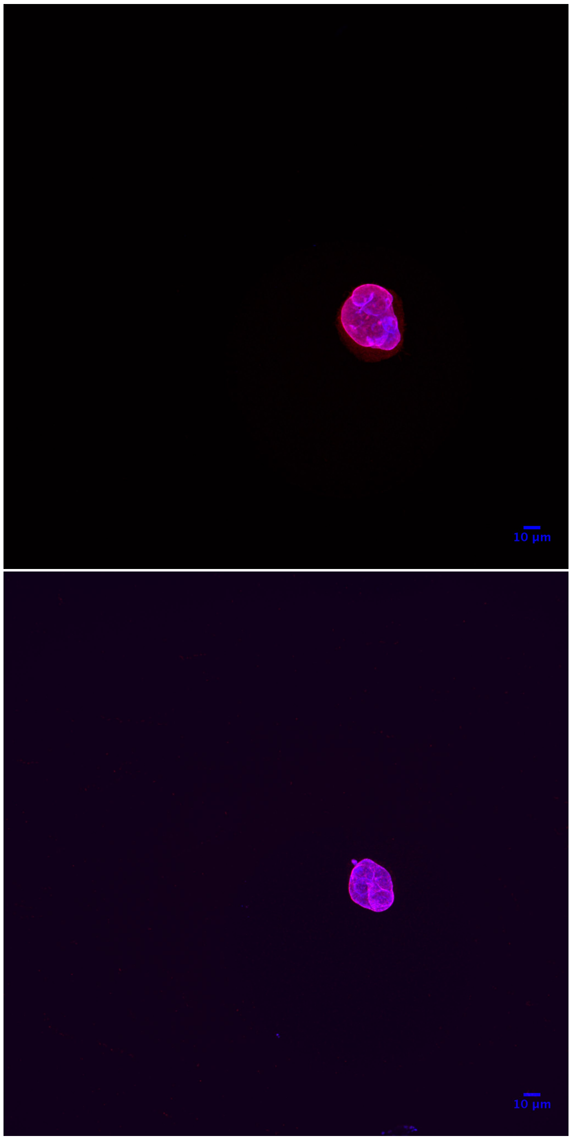

Figure 5-4: Cell gels expanded 4x and stained with intracellular markers. (Top) DAPI in blue and Histone H3 in magenta (Bottom) DAPI in blue and Histone H4 in red.

Chapter 6

Discussion

Recent advancements in scRNA-seq methods have enabled the discovery of new or rare cell types, revealed the mechanisms underlying cell development, and enabled us to probe the cellular ecosystem of diseases. However, to draw a complete picture of cellular heterogeneity, single cell protein information is necessary. Multiplexed transcriptomic and proteomic information will enable us to better understand correlations between mRNA and protein abundance, more precisely predict the target of therapeutics and analyze the effect of treatments. We present cell gels, a method to collect multiplexed mRNA and protein information in single cells. This method takes advantage of droplet barcoding and hydrogel chemistry to capture and barcode both mRNAs and proteins in thousands of cells.

Cell gels encapsulate live cells with barcoded beads, lysis buffer, monomer, and crosslinker in aqueous droplets. Polymerization is initiated after droplet collection by adding TEMED to droplets in bulk. While mRNAs are hybridized to DNA barcoded beads, proteins are crosslinked to the hydrogel matrix of cell gels. This arrangement allows us to make RNA libraries, measure proteins with antibodies, sort based on intracellular markers, expand cell gels, and other potential application.

Our experiments showed that acquisition of transcriptomic information from cell gels is challenging in several aspects. First, DTT, a common RNAse inhibitor, prevents polymerization by acting as a reducing agent. We tried inhibiting RNAse activity with HEPES and found that HEPES catalyzes polymerization significantly, making it unsuitable for our experiments. We settled on using GuHCl to inhibit RNAse activity.

Additionally, some of the differences in experimental results come from variability in different batches of beads. Differences in bead size also affect RNA-seq data, as smaller beads have a smaller oligo concentration per droplet. Lastly, in an attempt to understand the mechanisms affecting RNA-seq data quality, we conducted experiments to show that acrylamide and/or APS do not degrade RNA, but APS may interfere with reverse transcription.

In some of our experiments, we found that dissolving gels before cDNA amplification results in a complete loss of material. The average size of amplified cDNA of these samples without gel dissolution was shorter than expected. These evidences suggest that we may be capturing DNA in cell gels and amplifying it through nonspecific binding of SMART primers, rather than amplifying cDNA.

On the proteomic side, we have shown the possibility of capturing intracellular proteins in cell gels, staining with fluorophore conjugated antibodies, and sorting based on intracellular markers. We have also successfully expanded cell gels, with an expansion factor of 4x, and imaged the expanded samples with fluorescent intracellular markers.

To make cell gels a robust method for multiplexed measurements, the yield of RNA-seq data quality must first be improved. There are several experiments that can help in doing so. First, we hypothesize that polyacrylamide gels may interfere with hybridization to DNA barcoded beads or chemically modify the beads. Although the exact mechanisms of this interference is unknown to us, we suggest generating cell gels with alternative gels, such as poly(ethylene glycol) acrylate and poly(ethylene glycol) diacrylate (PEGDA), which gels rapidly in the presence of a photo-initiator and UV light. PEG gels have previously been used for nucleic acid studies [20] and could potentially resolve issues we have observed with bead based RNA-seq in acrylamide gels. Additionally, they eliminate the use of APS.

By hybridizing purified soluble RNA to beads prior to droplet generation and staining with SYTO RNAselect, a green fluorescent marker that selectively stains

RNA, we can more simply investigate whether RNA is degraded before reverse transcription. We could also use a strong RNAse inhibitor, such as SuperRase-In, in the lysis/bead solution to inhibit RNA degradation prior to reverse transcription.

Our current experiments prove the possibility of using cell gels as a method to detect the intracellular proteins in cells. However, there is more work to be done to quantify our measurements and enable barcoding proteins to map the barcodes to their cell of origin, which may be done with cleavable oligo conjugated antibodies.

Although our method requires improvements to enable obtaining transcriptome information, we have shown the use of cell gels as a platform for obtaining high-throughput proteomic information in single cells. Cell gels creates an environment that stably maintains intracellular molecules for months and eliminates the need for cell fixation. We hope that with further improvements, cell gels develops into a promising method for capturing multiplexed measurements of transcriptome and proteome in single cells.

Bibliography

[1]

[2] Shelley L Anna, Nathalie Bontoux, and Howard A Stone. Formation of dispersions using flow focusing in microchannels. *Citation: Appl. Phys. Lett*, 82(364), 2003.

[3] Alexis Battle, Zia Khan, Sidney H. Wang, Amy Mitrano, Michael J. Ford, Jonathan K. Pritchard, and Yoav Gilad. Impact of regulatory variation from rna to protein. *Science*, 347(6222):664–667, 2015.

[4] Xiaoming Chen, Tomasz Glawdel, Naiwen Cui, and Carolyn L. Ren. Model of droplet generation in flow focusing generators operating in the squeezing regime. *Microfluidics and Nanofluidics*, 18(5-6):1341–1353, may 2014.

[5] Zhong Chen, Jun Ling, and Daniel Gallie. RNase activity requires formation of disulfide bonds and is regulated by the redox state. *Plant Molecular Biology*, 55(1):83–96, may 2004.

[6] Spyros Darmanis, Caroline Julie Gallant, Voichita Dana Marinescu, Mia Niklasson, Anna Segerman, Georgios Flamourakis, Simon Fredriksson, Erika Assarsson, Martin Lundberg, Sven Nelander, Bengt Westermark, and Ulf Landegren. Simultaneous Multiplexed Measurement of RNA and Proteins in Single Cells. *Cell Reports*, 14(2):380–389, jan 2016.

[7] Cyrille L Delley, Leqian Liu, Maen F Sarhan, and Adam R Abate. Combined aptamer and transcriptome sequencing of single cells. *Scientific reports*, 8(1):2919, feb 2018.

[8] Allon M Klein, Linas Mazutis, Ilke Akartuna, Naren Tallapragada, Adrian Veres, Victor Li, Leonid Peshkin, David A Weitz, and Marc W Kirschner. Droplet barcoding for single-cell transcriptomics applied to embryonic stem cells. *Cell*, 161(5):1187–1201, may 2015.

[9] Melinda A Lake, Cody E Narciso, Kyle R Cowdrick, Thomas J Storey, Siyuan Zhang, Jeremiah J Zartman, and David J Hoelzle. Microfluidic device design, fabrication, and testing protocols.

[10] Yansheng Liu, Andreas Beyer, and Ruedi Aebersold. On the Dependency of Cellular Protein Levels on mRNA Abundance. *Cell*, 165(3):535–550, apr 2016.

[11] Evan Z. Macosko, Anindita Basu, Rahul Satija, James Nemesh, Karthik Shekhar, Melissa Goldman, Itay Tirosh, Allison R. Bialas, Nolan Kamitaki, Emily M. Martersteck, John J. Trombetta, David A. Weitz, Joshua R. Sanes, Alex K. Shalek, Aviv Regev, and Steven A. McCarroll. Highly parallel genome-wide expression profiling of individual cells using nanoliter droplets. *Cell*, 161(5):1202–1214, 2015.

[12] Linas Mazutis, John Gilbert, W Lloyd Ung, David A Weitz, Andrew D Griffiths, and John A Heyman. Single-cell analysis and sorting using droplet-based microfluidics. *Nature Protocols*, 8(5):870–891, apr 2013.

[13] Vanessa M Peterson, Kelvin Xi Zhang, Namit Kumar, Jerelyn Wong, Lixia Li, Douglas C Wilson, Renee Moore, Terrill K McClanahan, Svetlana Sadekova, and Joel A Klappenbach. Multiplexed quantification of proteins and transcripts in single cells. *Nature Biotechnology*, 35(10):936–939, aug 2017.

[14] Abbas H Rizvi, Pablo G Camara, Elena K Kandror, Thomas J Roberts, Ira Schieren, Tom Maniatis, and Raul Rabadan. Single-cell topological RNA-seq analysis reveals insights into cellular differentiation and development. *Nature Biotechnology*, 35(6):551–560, may 2017.

[15] Howard M. (Howard Maurice) Shapiro. *Practical flow cytometry.* Wiley-Liss, 2003.

[16] Marlon Stoeckius, Christoph Hafemeister, William Stephenson, Brian Houck-Loomis, Pratip K Chattopadhyay, Harold Swerdlow, Rahul Satija, and Peter Smibert. Simultaneous epitope and transcriptome measurement in single cells. *Nature Methods*, 14(9):865–868, jul 2017.

[17] Paul W. Tillberg, Fei Chen, Kiryl D. Piatkevich, Yongxin Zhao, Chih-Chieh Jay Yu, Brian P. English, Linyi Gao, Anthony Martorell, Ho-Jun Suk, Fumiaki Yoshida, Ellen M. DeGennaro, Douglas H. Roossien, Guanyu Gong, Uthpala Seneviratne, Steven R. Tannenbaum, Robert Desimone, Dawen Cai, and Edward S. Boyden. Protein-retention expansion microscopy of cells and tissues labeled using standard fluorescent proteins and antibodies. *Nature biotechnology*, (November 2015):1–9, 2016.

[18] Itay Tirosh, Benjamin Izar, Sanjay M Prakadan, Marc H Wadsworth, Daniel Treacy, John J Trombetta, Asaf Rotem, Christopher Rodman, Christine Lian, George Murphy, Mohammad Fallahi-Sichani, Ken Dutton-Regester, Jia-Ren Lin, Ofir Cohen, Parin Shah, Diana Lu, Alex S Genshaft, Travis K Hughes, Carly G K Ziegler, Samuel W Kazer, Aleth Gaillard, Kellie E Kolb, Alexandra-Chloé Villani, Cory M Johannessen, Aleksandr Y Andreev, Eliezer M Van Allen, Monica Bertagnolli, Peter K Sorger, Ryan J Sullivan, Keith T Flaherty, Dennie T Frederick, Judit Jané-Valbuena, Charles H Yoon, Orit Rozenblatt-Rosen, Alex K Shalek, Aviv Regev, and Levi A Garraway. Dissecting the multicellular ecosystem of metastatic melanoma by single-cell RNA-seq. *Science (New York, N.Y.)*, 352(6282):189–96, apr 2016.

[19] Alexandra-Chloé Villani, Rahul Satija, Gary Reynolds, Siranush Sarkizova, Karthik Shekhar, James Fletcher, Morgane Griesbeck, Andrew Butler, Shiwei Zheng, Suzan Lazo, Laura Jardine, David Dixon, Emily Stephenson, Emil Nilsson, Ida Grundberg, David McDonald, Andrew Filby, Weibo Li, Philip L De Jager, Orit Rozenblatt-Rosen, Andrew A Lane, Muzlifah Haniffa, Aviv Regev, and Nir Hacohen. Single-cell RNA-seq reveals new types of human blood dendritic cells, monocytes, and progenitors. *Science (New York, N.Y.)*, 356(6335):eaah4573, apr 2017.

[20] Liyi Xu, Ilana L Brito, Eric J Alm, and Paul C Blainey. Virtual microfluidics for digital quantification and single-cell sequencing. *Nature Methods*, 13(9):759–762, sep 2016.

[21] Grace X. Y. Zheng, Jessica M. Terry, Phillip Belgrader, Paul Ryvkin, Zachary W. Bent, Ryan Wilson, Solongo B. Ziraldo, Tobias D. Wheeler, Geoff P. McDermott, Junjie Zhu, Mark T. Gregory, Joe Shuga, Luz Montesclaros, Jason G. Underwood, Donald A. Masquelier, Stefanie Y. Nishimura, Michael Schnall-Levin, Paul W. Wyatt, Christopher M. Hindson, Rajiv Bharadwaj, Alexander Wong, Kevin D. Ness, Lan W. Beppu, H. Joachim Deeg, Christopher McFarland, Keith R. Loeb, William J. Valente, Nolan G. Ericson, Emily A. Stevens, Jerald P. Radich, Tarjei S. Mikkelsen, Benjamin J. Hindson, and Jason H. Bielas. Massively parallel digital transcriptional profiling of single cells. *Nature Communications*, 8:14049, jan 2017.

[22] Y. Y. Zhu, E. M. Machleder, A. Chenchik, R. Li, and P. D. Siebert. Reverse transcriptase template switching: A SMART approach for full-length cDNA library construction, 2001.